CrystEngComm

Cite this: *CrystEngComm*, 2011, **13**, 5292

www.rsc.org/crystengcomm

COMMUNICATION

Photo-induced nucleation of rutile nanorods—an ignored parameter in crystallization†

Tsung-Ying Ke,[a] Po-Chin Chen,[a] Min-Han Yang,[a] Hsin-Tien Chiu[c] and Chi-Young Lee*[ab]

Received 15th March 2011, Accepted 23rd June 2011
DOI: 10.1039/c1ce05317e

This work presents a surfactant-free and economical sol–gel method to synthesize multi-branched rutile TiO_2 nano-trees. Simple illumination by incandescent light during synthesis causes numerous branches to grow from the sides of nanorods, this process is accompanied by hydroxylation of the crystal surface. A {101} twin is demonstrated to connect the trunk to the branches. The extents of branching and surface hydroxylation are controlled by either photo-illumination or the addition of an exciton scavenger (H_2O_2). The relationship between the quantity of the branches and the excitons can be elucidated by considering photo-induced defects.

Rutile TiO_2, the most stable form of titanium dioxide, has been synthesized using the sol–gel process for decades, without the need for a traditional high temperature process. This stable material has been developed for several applications, such as gas sensors, lithium ion batteries, dielectric materials, field emission, photocatalysts, solar cells and others.[1–11] All of these uses depend strongly on the crystallinity of the material. Crystallographic shear (CS) structure is commonly formed in rutile TiO_2 by the accumulation of oxygen vacancies.[12–15] Among all dislocations, the $\langle 101 \rangle$ $[10\bar{1}]$ slip system resulting in CS structure is the most energetically favorable one. Such dislocations are also formed when a thin film grows epitaxially on another substrate with a large lattice mismatch.[14] In most cases, dislocations are unpredictable and difficult to control.

When formed in a sol–gel process, rutile TiO_2 usually is rod-shaped, with a preferred growth direction of $\langle 001 \rangle$, the diagonal of the rectangular cross-section along $\langle 100 \rangle$, and the exposed surfaces $\{110\}$.[7] The stability of the $\{110\}$ surface has made this material the great platform for studying surface chemistry. Also, its reactivity with H_2O_2 in photo-catalysis substantially increases the efficiency of the photo-catalytic decomposition of pollutants.[7,8] The efficiency not only increases in proportion to the effective surface area, which is determined by particle size and dispersion, but also depends on the structure of the surface, which may include, for example, surface hydroxyl groups or an exposed face. Hence, a rutile TiO_2 photo-catalyst should be nano-sized, have a wide open geometry, and an appropriate surface morphology.

Recently, some discoveries have been made about the synthesis of rutile TiO_2 with branched nano-structures, including 3-D branches. They were made using Ti metal as a substrate suspended in hydrothermal solution,[6] imperfect oriented attachment,[16] or by using titanate as a growth template.[17] 2-D V-shaped branches have been obtained using a chelating surfactant as a growth-directing agent.[18–21] These accidental branches connect with the trunk by sharing the $\{101\}$ twin plane, which is the most commonly observed CS plane. To promote green chemistry and mass production, a simple substitutive synthetic method without a surfactant is required.

Illumination with a light-bulb during the synthesis process can produce multi-branched rutile TiO_2 nanorods with a twin structure and surface hydroxylation. Typically, in the laboratory, a transparent glass reaction flask is adopted in the sol–gel process. Therefore, a series of experiments in which the variable parameter is illumination, which can be remotely controlled from outside the container, is designed.

The branched and un-branched rutile TiO_2 was synthesized by refluxing titanate in acid solution under different reaction conditions. The synthesis of titanate has been mentioned elsewhere.[7] A few grams of titanate was added to 1.0 M HCl solution in a Pyrex glass flask, and the mixture was refluxed at 150 °C for hours. The obtained precipitate was un-branched rutile nanorods. The branched rutile nanorods were synthesized similarly, except in that the transparent flask was illuminated from the outside by light bulbs or fluorescent tubes during the reaction. Afterward, a scanning electron microscope equipped with an energy dispersive X-ray spectroscope (EDS) was adopted to characterize the morphology and composition of the

[a]*Department of Materials Science and Engineering, National Tsing Hua University, Hsinchu, Taiwan, 30013, R. O. C; Fax: +886-3-5166687; Tel: +886-3-5742570*
[b]*Center for Nanotechnology, Materials Science, and Microsystems, National Tsing Hua University, Hsinchu, Taiwan, 30043, R. O. C. E-mail: cylee@mx.nthu.edu.tw; Fax: +886-3-5166687; Tel: +886-3-5742570*
[c]*Department of Applied Chemistry, National Chiao Tung University, Hsinchu, Taiwan, 30010, R. O. C*

† Electronic supplementary information (ESI) available: Fig. S1 presents the XRD results. Both branched (Fig. S1a) and un-branched (Fig. S1b) samples have the same crystalline phase, which is the rutile phase TiO_2 from the ICSD-9161 database (Fig. 2c). The diffractions at $2\theta = 27.4°$, 36.1°, and 54.4° correspond to (110), (101), and (211), respectively. Obviously, the intensity of the (101) and (002) signals of the one dimensional rutile rods is higher than those of the powder rutile patterns (Fig. S1c), owing to the preferred orientation of rutile rods. On the other hand, the intensity of these signals of the branched rutile is almost identical with those of the powder rutile, perhaps because more defects are present along the normal to the (101) plane of the branched rods than are present along the normal to the same plane of the unbranched rods. See DOI: 10.1039/c1ce05317e

samples. The crystal phase was identified by powder X-ray diffraction (XRD). A transmission electron microscope (TEM) was applied to analyze the detail crystal structure. The elements at the surface were semi-quantitatively analyzed by X-ray photo-electron spectroscopy (ESCA).

Fig. 1 presents the SEM images of the rutile nanorods with and without branches obtained in different reaction conditions. Fig. 1b reveals abundant three-dimensional branched nanorods that had been synthesized by refluxing titanate in 1 M HCl solution under illumination by an incandescent light bulb. The powder comprised particles with a main trunk and some branches; the angle between the branches and the trunk was around 114°, as presented in the inset image. However, normal sol–gel synthesis without photoillumination yielded one-dimensional unbranched nanorods as the precipitate, as displayed in Fig. 1a.[7] Also, according to EDX analysis (not shown), both samples, branched and un-branched, contain only Ti and O. Therefore, both the trunk and its branches of the branched sample and the one dimensional nanorods are titanium oxides. The XRD results present that both branched and un-branched samples have the same crystalline phase, which is the rutile phase TiO_2 from the ICSD-9161 database (ESI 1†).

Fig. 2 presents the TEM studies of the branched rutile rod. Fig. 2a presents the TEM image in which, when the zone axis is parallel to the [100] direction of the trunk, the angle between the trunk and the left branch is approximately 114°, as presented in Fig. 1b and c. Fig. 2b–d show the electron diffraction (ED) patterns that correspond to points b, c, d, respectively in Fig. 2a, with a ⟨100⟩ zone axis. The diffraction patterns at positions b and d are similar but rotated by ~114°, and Fig. 2c presents the diffraction pattern at position c which is the superimposition of those in Fig. 2b and d. This observation reveals that both the trunk and the left branch are separated single crystals with the same preferential growth direction parallel to the *c*-axis. According to the literature, the twinning of the {101} is most likely in the branched rutile. To determine the conjugated structure, a simulation is performed. As shown in the inset in Fig. 2a,

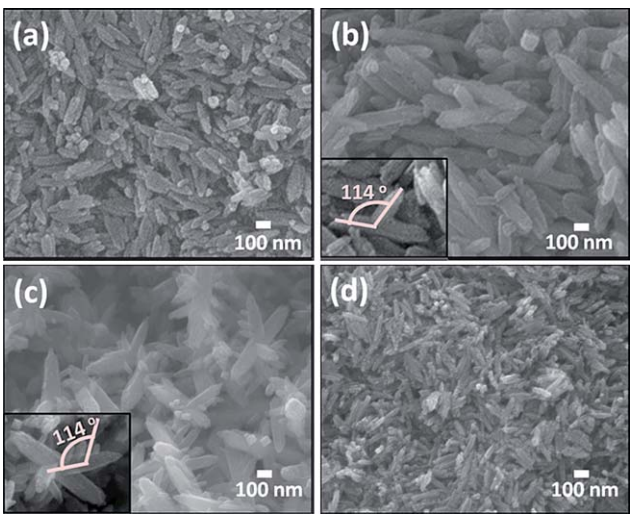

Fig. 1 SEM images of rutile TiO_2 rods synthesized in different reaction conditions in a: (a) normal sol–gel process, (b) sol–gel process under an incandescent light bulb illumination, (c) sol–gel process under 365 nm UV light illumination and (d) H_2O_2-added sol–gel process under an incandescent light bulb illumination. The inset in (b) and (c) presents nanorods at higher magnification.

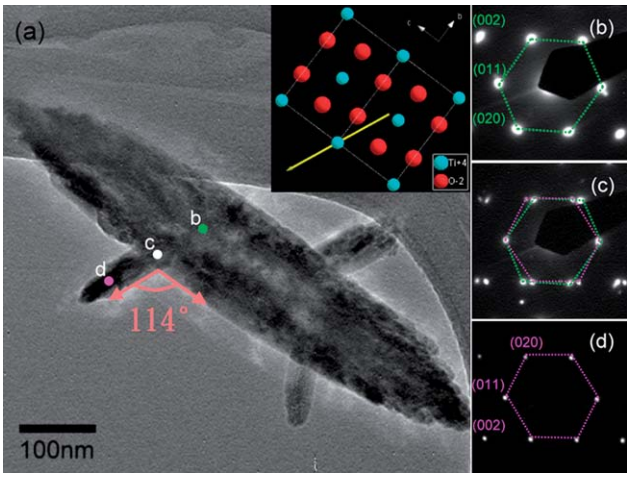

Fig. 2 (a) TEM image of multi-branched nanorod observed along the [100] direction of the trunk. (b), (c), and (d) Electron diffraction patterns obtained at points b, c, and d in part (a), respectively. The inset in (a) presents corresponding simulation, yellow arrow as the left branch and the lattice as the trunk.

when the {101} plane is set as the twin plane, the [100] direction of the trunk is set as the zone axis, and the *c*-axis is set as the growth direction, the measured angle is ~114°, consistent with the experimental observations. Further investigations have also been carried out to verify that all branches belonged to the same twin structure (ESI 2 and 3†).

Since the growth of branches violates the natural crystalline symmetry of tetragonal rutile, the appearance of the hierarchical structure is rare and normally accidental. Although numerous branched rutile TiO_2 materials have been reported by several research groups,[6,16–21] their growth mechanisms remain unknown. Generally in rutile TiO_2, each TiO_6 octahedron shares two opposing edges—each with an adjacent neighbor in a linear chain structure.[7] These chains lined up in alternating directions to form sheets of TiO_2. Three-dimensional rutile can be formed by the stacking of such sheets. In an acid catalyzed sol–gel process, condensation proceeds preferentially in the equatorial plane of the octahedrons, resulting in growth by edge sharing in the ⟨001⟩ direction, elongating the chains in these directions, forming fibril rutile. Titanium dioxide is known to be an effective material that is well known for its excellent photocatalytic ability. On excitation by a photon with energy equal to the up-band gap, electron–hole exciton pairs are formed and diffuse to different directions to the crystal surface. These excitons either react directly with incoming species (pollutants or H_2O) or react with surface ligands to form reactive radicals. In rutile TiO_2, the produced excitons diffuse to the surface and temporarily form defect sites, such as Ti^{3+} or oxygen vacancies, which become active sites for the dissociation of H_2O into surface hydroxyl groups[22–24] or surface peroxo intermediates for the photo-evolution of oxygen.[25]

Herein, surface oxygen associated with the defects that were formed under illumination was examined by XPS. Fig. 3 presents the O1s and Ti2p XPS spectra of rutile TiO_2 with and without branches. The O1s spectrum of TiO_2 without branches (Fig. 3a) that was formed in a normal sol–gel process included one major peak at around 530.9 eV, assigned to lattice oxygen (O_L) in bulk TiO_2, and a small shoulder peaked at about 532.5 eV, assigned to surface

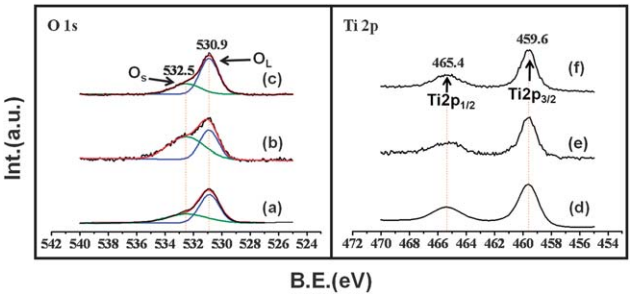

Fig. 3 O1s (a, b, and c) and Ti2p (d, e, and f) XPS spectra of TiO_2 formed in: (a and d) normal sol–gel process, (b and e) sol–gel process under illumination, and (c and f) sol–gel process under illumination with H_2O_2 added.

Table 1 Estimated XPS peak areas of different rutile TiO_2 obtained under various reaction conditions

	a	*b*	*c*
O_L (530.9 eV)	0.78	0.81	0.63
O_S (532.5 eV)	0.49	1.21	0.39
Ti (459.6 eV)	1	1	1

[a] Normal sol–gel process. [b] Sol–gel process under light illumination. [c] H_2O_2-added sol–gel process under light illumination. O1s peak areas are normalized with respect to their corresponding Ti2p peak areas.

oxygen (O_S).[26] In contrast, in Fig. 3b, the spectrum of branched TiO_2 that was formed in a photo-assisted process includes two O1s peaks at approximately 530.9 and 532.5 eV, which are of similar intensity. The Ti2p spectra of various forms of TiO_2 included only lattice Ti^{4+} signals (as displayed in Fig. 3d–f), and no shift was observed. The areas under the peaks are estimated by semi-quantitative analysis and the results are presented in Table 1.

H_2O_2, normally acts as an electron scavenger[7,8] in photocatalysis. It is applied herein to clarify the relationship between photo-excited excitons and branch formation. When 10 mM H_2O_2 is added to the reaction solution, rutile nanorods without branches are obtained under illumination (Fig. 1d). Further prolonging the reaction time until all of the H_2O_2 had been exhausted under the influence of both heat and light, branched rutile appeared again. Also, the O1s XPS spectrum of the TiO_2 obtained by illumination in the H_2O_2 solution reveals lattice oxygen atoms with a few surface oxygen atoms. Apparently, as electrons were removed by H_2O_2, the accumulation of holes in the lattice was prohibited, so dislocations such as twins cannot form. Briefly, when rutile TiO_2 was synthesized under illumination, holes were trapped at surface sites to form surface oxygen; electrons were trapped in the non-stoichiometric {101} mirror plane, producing oxygen vacancies, leading to the formation of extra titanium layers, which result in the formation of defects such as vacancies, edge-dislocations, and further leading to twin formation.[12–15]

In an experiment, a fluorescent tube with a peak wavelength of 365 nm (close to the TiO_2 band gap) was adopted as a light source, and many branched nanorods with numerous branches were obtained. Fig. 1c presents an SEM image of a multi-branched nanorod with primary and secondary branches. The branches appear to penetrate the trunk. Obviously, during photo-assisted synthesis, defects that were formed by illumination acted as nucleation sites for branch growth. Scheme 1 describes their proposed growth sequence.

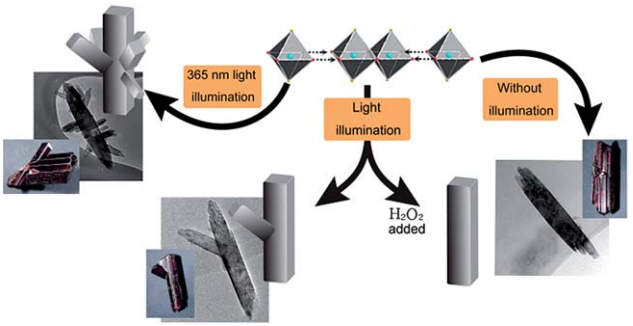

Scheme 1 Growth sequence of branched and un-branched rutile TiO_2 rods by acid treated titanate at 150 °C. The pictures in the corner are the rutile TiO_2 obtained from ore.[27]

In summary, a multi-branched rutile TiO_2 nanostructure was synthesized in a photo-assisted sol–gel process. The branches are suggested to have been formed owing to nucleation on the defect inducing twin plane. The appearance of surface oxygen atoms, revealed by XPS measurements of branched rutile TiO_2, establishes the photo-excited growth pathway. The amount of branches can be varied by controlling the quantity of excitons that are produced by adjusting the illumination or the use of exciton scavenger. This work describes a simple method for manipulating crystal growth behaviors, including branch growth and surface hydroxylation, without changing the precursor concentration or synthesis temperature. The newly identified phenomena, caused by light—especially those of photo-catalytic materials—may be useful in the synthesis of various materials.

Notes and references

1 M. Sanchez and M. E. Rincon, *Sens. Actuators, B*, 2009, **140**, 17–23.
2 Y. S. Hu, L. Kienle, Y. G. Guo and J. Maier, *Adv. Mater.*, 2006, **18**, 1421–1426.
3 S. K. Kim, W. D. Kim, K. M. Kim, C. S. Hwang and J. Jeong, *Appl. Phys. Lett.*, 2004, **85**, 4112–4114.
4 K. F. Huo, X. M. Zhang, L. S. Hu, X. J. Sun, J. J. Fu and P. K. Chu, *Appl. Phys. Lett.*, 2008, **93**, 13105.
5 T. Paunesku, T. Rajh, G. Wiederrecht, J. Maser, S. Vogt, N. Stojicevic, M. Protic, B. Lai, J. Oryhon, M. Thurnauer and G. Woloschak, *Nat. Mater.*, 2003, **2**, 343–346.
6 X. F. Yang, J. Zhuang, X. Y. Li, D. H. Chen, G. F. Ouyang, Z. Q. Mao, Y. Han, Z. H. He, C. L. Liang, M. M. Wu and J. C. Yu, *ACS Nano*, 2009, **3**, 1212–1218.
7 T. Y. Ke, C. W. Peng, C. Y. Lee, H. T. Chiu and H. S. Sheu, *CrystEngComm*, 2009, **11**, 1691–1695.
8 R. Scotti, M. D'Arienzo, A. Testino and F. Morazzoni, *Appl. Catal., B*, 2009, **88**, 497–504.
9 X. M. Song, J. M. Wu, M. Z. Tang, B. Qi and M. Yan, *J. Phys. Chem. C*, 2008, **112**, 19484–19492.
10 J. H. Bang and P. V. Kamat, *Adv. Funct. Mater.*, 2010, **20**, 1970–1976.
11 X. M. Song, J. M. Wu, L. Meng and M. Yan, *J. Am. Ceram. Soc.*, 2010, **93**, 2068–2073.
12 J. G. Zheng, X. Q. Pan, M. Schweizer, F. Zhou, U. Weimar, W. Göpel and M. Rühle, *J. Appl. Phys.*, 1996, **79**, 7688–7694.
13 D. G. Rickerby and M. C. Horrillo, *Nanostruct. Mater.*, 1998, **10**, 357–363.
14 H. Wakabayshi, T. Suzuki, Y. Iwazaki and M. Fujimoto, *Jpn. J. Appl. Phys.*, 2001, **40**, 6081–6087.
15 G. Wang and G. Li, *Eur. Phys. J. D*, 2003, **24**, 355.
16 M. H. Tsai, S. Y. Chen and P. Shen, *Nano Lett.*, 2004, **4**, 1197–1201.
17 X. F. Yang, C. Karthik, X. Y. Li, J. X. Fu, X. H. Fu, C. L. Liang, N. Ravishankar, M. M. Wu and G. Ramanath, *Chem. Mater.*, 2009, **21**, 3197–3201.

18 C. C. Weng, K. F. Hsu and K. H. Wei, *Chem. Mater.*, 2004, **16**, 4080–4086.
19 J. M. Wu, B. Huang, M. Wang and A. Osaka, *J. Am. Ceram. Soc.*, 2006, **89**, 2660–2663.
20 J. M. Wu and B. Qi, *J. Phys. Chem. C*, 2007, **111**, 666–673.
21 W. Sun, S. Zhou, P. Chen and L. Penga, *Chem. Commun.*, 2008, 603–605.
22 S. n. Wendt, P. T. Sprunger, E. Lira, G. K. H. Madsen, Z. S. Li, J. Ø. Hansen, J. Matthiesen, A. Blekinge-Rasmussen, E. Lægsgaard, B. Hammer and F. Besenbacher, *Science*, 2008, **320**, 1755–1759.
23 N. G. Petrik, Z. R. Zhang, Y. G. Du, Z. Dohnálek, I. Lyubinetsky and G. A. Kimmel, *J. Phys. Chem. C*, 2009, **113**, 12407–12411.
24 Z. Zhang, J. S. Lee, J. T. Yates, Jr, R. Bechstein, E. Lira, J. Ø. Hansen, S. Wendt and F. Besenbacher, *J. Phys. Chem. C*, 2010, **114**, 3059–3062.
25 R. Nakamura and Y. Nakato, *J. Am. Chem. Soc.*, 2004, **126**, 1290–1298.
26 G. Ketteler, S. Yamamoto, H. Bluhm, K. Andersson, D. E. Starr, D. F. Ogletree, H. Ogasawara, A. Nilsson and M. Salmeron, *J. Phys. Chem. C*, 2007, **111**, 8278–8282.
27 http://www.mineralminers.com/html/rutmins.stm.